

Effect of friction stress of droplets with film on prediction of pressure changes in condensing tubes

H. Saffari*, N. Dalir**

*School of Mechanical Engineering, Iran University of Science and Technology (IUST), Tehran, Iran, 16887,

E-mail: saffari@iust.ac.ir

**School of Mechanical Engineering, Iran University of Science and Technology (IUST), Tehran, Iran, 16887,

E-mail: ne.dalir@gmail.com

crossref <http://dx.doi.org/10.5755/j01.mech.17.1.203>

Nomenclature

A - channel cross-sectional area, m^2 ; a - interfacial area concentration, m^{-1} ; C_D - drag coefficient; D - diameter, m ; f - friction coefficient; G - mass flux, kg/m^2s ; g - gravitational constant, m/s^2 ; h - specific enthalpy, J/kg ; h_{fg} - latent heat of vaporization, J/kg ; k - thermal conductivity, $W/(mK)$; l - length, m ; M - source terms in balance equations; m - mass, kg ; P - pressure, Pa ; Δp - pressure drop, Pa ; Pr - Prandtl number ($Pr = \mu C_p/k$); Q - volumetric flow rate, m^3/s ; q_V - volumetric heat flux, W/m^3 ; Re - Reynolds number ($Re = \rho U l/\mu$); S - perimeter, m ; T - temperature, K ; t - time, s ; u - velocity, m/s ; x - coordinate, m ; W_d - deposition rate of entrained droplets, kg/m^2s ; W_e - droplets entrainment rate, kg/m^2s ; We - Weber number.

Greek symbols

Γ - evaporation/condensation rate, kg/m^3s ; α - volume fraction; δ - liquid film thickness, m ; θ - angle of tube inclination, rad ; μ - dynamic viscosity, kg/ms ; ν - kinematic viscosity, m^2/s ; ρ - density, kg/m^3 ; σ - surface tension, N/m ; τ - shear stress, N/m^2 ; τ_e - evaporation relaxation time, s ; τ_c - condensation relaxation time, s .

Subscripts

D - droplet, h - hydraulic parameter, k - phase indicator, 0 - initial conditions, 1 - gas, 2 - liquid film, 3 - entrained droplets, W - wall.

1. Introduction

Steam condensation inside vertical tubes is applied in various heat exchangers in power and chemical industry. For instance, an important task in the design of an air heater is to predict the pressure change along the downward flow of condensing steam inside the tube. This pressure change determines the pressure of condensate at the condensing tube outlet and the pressure drop that must be provided in order to remove the drained condensate from the outlet header to the condensate line for its removal.

For condensation inside vertical or near vertical tubes, annular flow is the dominant flow regime. To analyze this condensation mechanistic (phenomenological) models have often been used. One of these phenomenological models is the two-fluid model, in which the liquid film flowing adjacent to the wall and the gas phase flowing in the tube cross-section core comprise the two fluids. However, the two-fluid model is not complete because it is reported that in condensation the droplets entrain from the liquid film to the gas core and deposit from the gas core to the liquid film [1]. Thus, there is another fluid flowing

inside the gas core, which is due to the entrained droplets (or the dispersed phase). This introduces the three-fluid model, which comprises the gas phase in the tube cross-section core ($k = 1$), the liquid film flowing adjacent to the wall ($k = 2$) and the entrained droplets (dispersed phase, $k = 3$) flowing inside the gas phase (or vapor core). The three-fluid model functions reasonably well for condensation inside vertical tubes.

To attain such goal, the conservation equations of mass, momentum and energy are written for each fluid (with the index k), then steady one-dimensional conditions are considered (the one-dimension is along the tube length or along the condensation direction). Apart from nine conservation equations (mass, momentum and energy equations for $k = 1, 2, 3$), another equation is obtained from the fact that the sum of the volume fractions of the three fluids must be unity. These ten equations are used to obtain ten unknowns (ten state variables). In the conservation equations, the interfacial transfer phenomena between the fluid pairs that are in contact and also between the liquid film and wall are calculated by suitable closure relations.

The conservation equations along with volume fraction equation are changed, by some arithmetic operations, to ten first-order ordinary differential equations (ODEs) which give the derivatives of ten variables (parameters or state variables). These ten ODEs comprise a system of ODEs which should be solved together as they are coupled. When dealing with condensation, the ODE system is stiff. It means that while one of the state variables has a very limited range of variation (for example α), there is another state variable which varies in a large range (for example p) and so stiff ODE solvers should be used. Here for the solution of system of stiff ODEs, MATLAB stiff ODE solvers, namely ode23s and ode15s have been used. In the numerical procedure, the initial conditions are flow parameters at the inlet of the condensing tube (dependent variables $h_{k,0}$, $\alpha_{k,0}$, $u_{k,0}$, p_0).

The problem is that a downward flowing pure and saturated water vapor (steam) enters to a vertical tube with known initial conditions and condensation of the steam happens inside the vertical tube (Fig. 1). The flow regime is annular and entrainment and deposition are not negligible. Then a three-fluid model is developed to predict the pressure changes in the tube. Use of the previous correlations for the steam-liquid film interfacial friction shows discrepancies between calculated and measured (experimental) pressure changes. Although the correlation of Stevanovic et al. [2] provides good agreement, it has some deficiencies. One of these deficiencies corrected in this paper is introduction of the friction stress between en-

trained droplets and liquid film. Calculated pressure changes provide even much better agreement by taking the above correction into account.

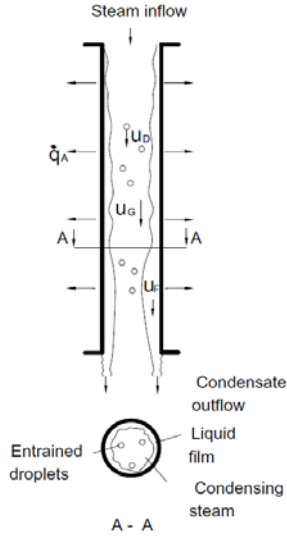


Fig. 1 Fluid streams in condensing vertical tube [2]

2. Modeling approach

2.1. Governing equations

The three-fluid model conservation equations

$$\frac{du_k}{dx} = \frac{u_k M_k - \rho_k u_k^2 \frac{d\alpha_k}{dx} - \alpha_k u_k^2 \frac{\partial \rho_k}{\partial p} \frac{dp}{dx} - \alpha_k u_k^2 \frac{\partial \rho_k}{\partial h_k} \frac{dh_k}{dx}}{\alpha_k \rho_k u_k} \quad (6)$$

$$\frac{d\alpha_k}{dx} = \alpha_k \frac{1 - u_k^2 \frac{\partial \rho_k}{\partial p} \frac{dp}{dx}}{\rho_k u_k^2} - \frac{M_{3+k} - 2u_k M_k + \alpha_k u_k^2 \frac{\partial \rho_k}{\partial h_k} \frac{dh_k}{dx}}{\rho_k u_k^2} \quad (7)$$

$$\frac{dp}{dx} = \frac{\sum_{k=1}^3 \frac{M_{3+k} - 2u_k M_k + \alpha_k u_k^2 \frac{\partial \rho_k}{\partial h_k} \frac{dh_k}{dx}}{\rho_k u_k^2}}{\sum_{k=1}^3 \alpha_k \frac{1 - u_k^2 \frac{\partial \rho_k}{\partial p}}{\rho_k u_k^2}} \quad (8)$$

The final set of balance equations are equations (5) - (8). These equations are implemented in the

Momentum balance source terms:

$$\left. \begin{aligned} \text{Gas flow :} & \quad M_4 = (-a_{12}\tau_{12} - a_{13}\tau_{13}) + (\Gamma_{21}u_2 - \Gamma_{12}u_1) + \\ & \quad + (\Gamma_{31}u_3 - \Gamma_{13}u_1) - \alpha_1 \rho_1 g \sin \theta \\ \text{Liquid film :} & \quad M_5 = (a_{12}\tau_{12} - a_{2W}\tau_{2W}) + (\Gamma_{12}u_1 - \Gamma_{21}u_2) + \\ & \quad + a_{12}(W_d u_3 - W_e u_2) - \alpha_2 \rho_2 g \sin \theta + a_{12}\tau_{23} \\ \text{Entrained Droplets :} & \quad M_6 = a_{13}\tau_{13} + (\Gamma_{13}u_1 - \Gamma_{31}u_3) - \\ & \quad - a_{12}(W_d u_3 - W_e u_2) - \alpha_3 \rho_3 g \sin \theta - a_{12}\tau_{23} \end{aligned} \right\} \quad (10)$$

have the following general form for steady one-dimensional flow conditions [1, 2]

$$\frac{d(\alpha_k \rho_k u_k)}{dx} = M_k \quad (1)$$

$$\frac{d(\alpha_k \rho_k u_k^2)}{dx} + \alpha_k \frac{dp}{dx} = M_{3+k} \quad (2)$$

$$\frac{d(\alpha_k \rho_k h_k u_k)}{dx} = M_{6+k} \quad (3)$$

where M represents mass, momentum and energy source terms as presented below, and index $k=1$ denotes gas phase, $k=2$ liquid film and $k=3$ entrained droplets. The volume balance is added as

$$\sum_{k=1}^3 \alpha_k = 1 \quad (4)$$

(This means that the sum of volume fractions of the fluids must be unity). The above system of conservation equations is transformed into a form suitable for the numerical integration as follows [2]

$$\frac{dh_k}{dx} = \frac{M_{6+k} - h_k M_k}{\alpha_k \rho_k u_k} \quad (5)$$

MATLAB code in the order of (5), (8), (7) and (6) and solved as an initial value problem where the initial conditions are the parameters values at tube inlet.

The source terms in conservation equations are as follows [2, 3]:

Mass balance source terms:

$$\left. \begin{aligned} \text{Gas flow :} & \quad M_1 = (\Gamma_{21} - \Gamma_{12}) + (\Gamma_{31} - \Gamma_{13}) \\ \text{Liquid film :} & \quad M_2 = (\Gamma_{12} - \Gamma_{21}) + a_{12}(W_d - W_e) \\ \text{Entrained Droplets :} & \quad M_3 = (\Gamma_{13} - \Gamma_{31}) - a_{12}(W_d - W_e) \end{aligned} \right\} \quad (9)$$

Energy balance source terms:

$$\left. \begin{aligned} \text{Gas flow :} & \quad M_7 = (\Gamma_{21} + \Gamma_{31})h_{g,sat} - (\Gamma_{12} + \Gamma_{13})h_{l,sat} \\ \text{Liquid film :} & \quad M_8 = \Gamma_{12}h_{l,sat} - \Gamma_{21}h_{g,sat} + a_{12}(W_d h_3 - W_e h_2) + \dot{q}_{V,2} \\ \text{Entrained Droplets :} & \quad M_9 = \Gamma_{13}h_{l,sat} - \Gamma_{31}h_{g,sat} - a_{12}(W_d h_3 - W_e h_2) \end{aligned} \right\} \quad (11)$$

with $h_{l,sat} = h_f(p)$, $h_{g,sat} = h_g(p)$.

2.2. Constitutive equations and comments

The deposition rate W_d , is calculated at each position from the relationship $W_d = k_d C$. k_d and C are estimated from the following correlation (Sugawara correlation [3])

$$k_d = 0.009u_1(C/\rho_1)^{-0.5} Re_1^{-0.2} Sc_1^{-2/3} \quad (12)$$

$$C = \frac{\dot{m}_3}{\dot{m}_1 u_3 / (\rho_1 u_1) + \dot{m}_3 / \rho_3} \quad (13)$$

The entrainment rate W_e , is estimated from the following correlation (Sugawara correlation [3])

$$W_e = 1.07 \frac{\tau_{21} \Delta h_{eq}}{\sigma} \frac{u_1 \mu_3}{\sigma} \left(\frac{\rho_3}{\rho_1} \right)^{0.4} \quad (14)$$

with

$$\Delta h_{eq} = k_s, \quad Re_1 > 10^5$$

$$\Delta h_{eq} = k_s [2.136 \log(Re_1) - 9.68], \quad Re_1 < 10^5$$

where

$$k_s = 0.57\delta + 21.73 \times 10^3 \delta^2 - 38.8 \times 10^6 \delta^3 + 55.68 \times 10^9 \delta^4.$$

The shear stress between the wall and liquid film is defined as

$$\tau_{2W} = f_{2W} \frac{\rho_2 |u_2| u_2}{2} \quad (15)$$

where the liquid film-wall interfacial friction coefficient and the liquid film Reynolds number are

$$f_{2W} = \frac{C}{Re_2^n}, \quad Re_2 = \frac{\rho_2 u_2 D_{h,2}}{\mu_2} \quad (16)$$

for turbulent flow (Blasius correlation, [4, 5]), $C = 0.079$, $n = 0.25$, $Re_2 > 1600$, and for laminar flow, $C = 16$, $n = 1$, $Re_2 \leq 1600$.

The liquid film - gas phase shear stress is defined as

$$\tau_{12} = f_{12} \frac{\rho_1}{2} |u_1 - u_2| (u_1 - u_2) \quad (17)$$

Correlations for gas phase-liquid film interfacial friction coefficient are as follows:

Modified Wallis correlation [6]

$$f_{12} = \frac{0.079}{Re_1^{0.25}} \left(1 + 300 \frac{\delta}{D} \right) \quad (18)$$

and Reynolds number for the gas flow is $Re_1 = \frac{\rho_1 u_1 D_{h,13}}{\mu_1}$.

Alipchenkov et al. correlation [7]

$$f_{12} = \frac{0.25}{(1.82 \log Re_1 - 1.64)^2} + 1.5 \frac{\delta}{D} \quad (19)$$

where Re_1 is defined as in case of Wallis correlation.

Levitan correlation [8]

$$f_{12} = 0.001 \left(\frac{\rho_2}{\rho_1} \right)^{0.4} \left(1 + 300 \frac{\delta}{D} \right) \quad (20)$$

Stevanovic et al. correlation [2]

$$f_{12} = \frac{0.079}{Re_1^{0.25}} + 46.35 \frac{\delta}{D} \left(\frac{\rho_1}{\rho_2} \right)^{0.8} \quad (21)$$

The gas phase- droplets shear stress is defined as

$$\tau_{13} = \frac{1}{8} C_D \rho_1 |u_1 - u_3| (u_1 - u_3) \quad (22)$$

where the drag coefficient is (Clift et al. [9])

$$C_D = \frac{24}{Re_D} \left(1 + 0.15 Re_D^{0.687} \right) + \frac{0.42}{1 + 4.25 \times 10^4 Re_D^{-1.16}} \quad (23)$$

and the droplet Reynolds number is $Re_D = \frac{|u_1 - u_3| D_D \rho_1}{\mu_1}$.

The mean droplet diameter is determined by critical Weber number [10]

$$\left. \begin{aligned} D_D &= 10^{-4} m, \quad Y \leq 10^{-4} \\ D_D &= Y, \quad 10^{-4} < Y < 3 \times 10^{-3} \\ D_D &= 3 \times 10^{-3}, \quad Y \geq 3 \times 10^{-3} \end{aligned} \right\} \quad (24)$$

where we have $Y = \frac{\sigma We}{\rho_1 (u_1 - u_3)^2}$, and $We = 0.799$.

Evaporation and condensation rate. To the calculation of the evaporation rate the nonequilibrium relaxation method is used, whereby it is assumed that during flashing (pressure undershoots) the volumetric evaporation rate follows [11, 12]:

Evaporation rate:

$$\left. \begin{aligned} \Gamma_{k1} &= \frac{\alpha_k \rho_k}{\tau_e} \frac{h_k - h'}{r}; \text{ for } h_k > h', \quad k = 2, 3 \\ \Gamma_{k1} &= 0; \text{ for } h_k \leq h' \end{aligned} \right\} \quad (25)$$

Condensation rate

$$\left. \begin{aligned} \Gamma_{1k} &= \frac{\alpha_k \rho_k}{\tau_c} \frac{h' - h_k}{r}; \text{ for, } h' > h_k, k = 2, 3 \\ \Gamma_{1k} &= 0; \text{ for, } h' \leq h_k \end{aligned} \right\} \quad (26)$$

where $\tau_e = \tau_c = -0.99(1 - \alpha_1) + 1$ are phase change relaxation times and also we have $r = h_{fg}(p)$, $h' = h_f(p) = h_{l,sat}(p)$.

Interfacial area concentrations are calculated between liquid film-wall, liquid film-gas and droplets-gas [13].

The tube flow cross section is $A = \pi D^2/4$ and the liquid film-wall perimeter and the liquid film-gas phase perimeter are

$$S_{2W} = \pi D, \quad S_{12} = \pi D \sqrt{1 - \alpha_2} \quad (27)$$

The liquid film-wall interfacial area concentration is

$$a_{2W} = \frac{S_{2W}}{A} = \frac{4}{D} \quad (28)$$

The liquid film-gas interfacial area concentration is

$$a_{12} = \frac{S_{12}}{A} = \frac{4\sqrt{1 - \alpha_2}}{D} \quad (29)$$

Droplets-gas interfacial area concentration is

$$a_{13} = 6 \frac{\alpha_3}{D_D} \quad (30)$$

where D_D is the droplet mean diameter.

The mean liquid film thickness is $\delta = 0.5D(1 - \sqrt{1 - \alpha_2})$.

The hydraulic diameter of the gas phase core is

$$D_{h,13} = \frac{4(1 - \alpha_2)A}{S_{12}} = D\sqrt{1 - \alpha_2} \quad (31)$$

Also the hydraulic diameter of the liquid film flow is

$$D_{h,2} = \frac{4\alpha_2 A}{S_{2W}} = D\alpha_2 \quad (32)$$

Friction stress of droplets with liquid film. The correction considered in this paper for the three-fluid model prediction of pressure changes in condensing vertical tubes assuming annular flow is the introduction of the friction stress between droplets and liquid film. The model attained is named the modified three-fluid model, which is in fact the correlation of Stevanovic et al. for gas phase-liquid film interfacial friction coefficient with correction - friction stress of droplets with film. To evaluate the friction stress of the droplets with the film, τ_{23} , we can invoke the

correlation between the intensities of turbulent fluctuations of the velocities of the dispersed (droplets) and carrier (liquid film) phases in the approximation of homogeneous turbulence [14]

$$\langle v'^2 \rangle = f_u \langle u'^2 \rangle, \quad f_u = \frac{1 + A\tau_u / T_{Lp}}{1 + \tau_u / T_{Lp}}, \quad A = \frac{(1 + C_{vm})\rho_1 / \rho_3}{1 + C_{vm}\rho_1 / \rho_3} \quad (33)$$

where $\langle v'^2 \rangle$ and $\langle u'^2 \rangle$ are the intensities of velocity fluctuations of the dispersed and carrier phases, f_u is the coefficient of response of the particles to the turbulent velocity fluctuations of the carrier phase and T_{Lp} is the time of interaction between the particles and the energy-containing eddies. The above equation is used to derive the following formula for the droplets-film friction stress

$$\tau_{23} = \frac{\alpha_3 \rho_3 (u_3 - u_2)^2}{\alpha_1 \rho_1 (u_1 - u_2)^2} f_u \tau_{12} \quad (34)$$

The eddy-droplet interaction time is determined by the following approximations [15]

$$T_{Lp} = T_{Lp}(St = 0) + [T_{Lp}(St = \infty) - T_{Lp}(St = 0)]F(St)$$

$$T_{Lp}(St = 0) = T_L \frac{4(3\beta + 3\beta^2/2 + 1/2)}{5\beta(1 + \beta)^2}, \quad \beta = \sqrt{1 + \gamma^2 + \frac{2\gamma}{\sqrt{3}}}$$

$$T_{Lp}(St = \infty) = T_L \frac{6(2 + \gamma)}{5(1 + \gamma)^2} \quad (35)$$

$$F(St) = \frac{St}{1 + St} - \frac{5St^2}{4(1 + St)^2(2 + St)}$$

here $St \equiv \tau_u / T_E$ is the Stokes number that quantifies the droplet inertia and thereby measures the degree of coupling between the gas and dispersed phases, T_L is Lagrangian integral time scale of turbulence, T_E is Eulerian time macroscale of turbulence in the moving coordinate system, $\gamma = |u_1 - u_2| / u_{1*}$ is the drift parameter, and $u_{1*} = \sqrt{\tau_{12} / \rho_1}$ is the friction velocity. As it follows from (35), for inertialess particles ($St = \gamma = 0$), T_{Lp} coincides with the Lagrangian time scale T_L . In the absence of the mean drift ($\gamma = 0$), T_{Lp} monotonically increases with increasing St from the Lagrangian time scale T_L for $St = 0$ to the Eulerian macroscale for $St = 1$. As the drift parameter γ increases, T_{Lp} decreases monotonically. The time scales of turbulence averaged over the channel cross-section are taken as $T_L = 0.04D_{h,13} / u_{1*}$ and $T_E = 0.1D_{h,13} / u_{1*}$, where $D_{h,13} = D\sqrt{1 - \alpha_2}$ is the equivalent diameter of the gas-dispersed core. τ_u is the dynamic response time of a droplet and is given as $\tau_u = \frac{4(\rho_3 + C_{vm}\rho_1)D_D}{3\rho_1 C_D |u_1 - u_3|}$, here C_D is the droplet drag coefficient (determined in τ_{13}), $C_{vm} = 0.5$ is the

virtual mass coefficient and D_D is the droplet mean diameter.

Virtual Mass Force. The virtual mass force occurs only when one of the phases accelerates with respect to the other phase. It results from the fact that the motion of the discontinuous phase results in the acceleration of the continuous phase as well. In terms of magnitude, the virtual mass force is significant only if the gas phase is dispersed, and only in rather extreme flow acceleration conditions (e.g., choked flow) [1].

In condensing vertical tubes, the virtual mass force is in fact a measure of the influence of the velocity of the entrained droplets on the velocity of the gas phase. Here the gas phase flow is continuous and the flow of the entrained droplets is dispersed, and therefore the magnitude of the virtual mass force is not significant, and so it is not considered.

3. Results and discussion

The experimental data are obtained from Kreydin et al. [16]. The tube diameter is 0.0132 m and the tube length is 2.93 m. Total pressure changes in condensing annular flow are shown in terms of the total mass flux (or steam inlet mass flux, G). The range of changes of G is from 0 to 500 kg/m²s and in the written code in MATLAB, the values of 0, 50, 100, 150, 200, 300, 400 and 500 kg/m²s are implemented. The cooling heat flux applied to the tube wall for condensing the steam is uniform (constant) along the tube length. In the cases of mass fluxes of 300 kg/m²s and 500 kg/m²s, the condensing heat fluxes are -68 W/cm² and -112 W/cm² respectively. The condensation of steam takes place inside the tube, i.e., pure saturated steam enters the tube and sub-cooled water (and saturated steam) exits the tube. Therefore, as the tube length is constant, the mass flux is proportional to the condensing heat flux, i.e., the higher mass fluxes mean the higher condensing heat fluxes.

In the present study, the calculated (by three-fluid model) and measured (experiments by Kreydin et al. [16]) total pressure changes (differences between outlet and inlet pressures) are plotted against the total mass fluxes (steam inlet mass fluxes) for different steam-liquid film interfacial friction correlations and the steam inlet pressure of 1.08 MPa in Fig. 2. As it can be seen, the modified three-fluid model (correlation of Stevanovic et al. [2] with proposed correction - introduction of shear stress of droplets with liquid film) provides much better agreement with the experimental data of Kreydin et al. [16]. The average value of absolute error for the predictions of the modified three-fluid model is 0.0678 kPa while the average value of absolute error for the predictions of the Stevanovic et al. correlation is 0.1429 kPa. Also the relative difference of the results of the modified three-fluid model with experimental data is 20% and the relative difference of the data of Stevanovic et al. correlation with experimental results is 50%. Therefore, the agreement of the results of the modified three-fluid model with experimental data is 30% better than the agreement of the results of Stevanovic et al. correlation with experimental data. It should be noted that the main difference between the modified three-fluid model and Stevanovic et al. correlation is in the region with total mass fluxes higher than approximately 120 kg/m²s, where the modified three-fluid model predicts higher total pres-

sure changes than Stevanovic et al. correlation (there is no experimental data of Kreydin et al. [16] for this region).

In this paper, the modified three-fluid model predictions are compared only with predictions of Stevanovic et al. correlation because among the available correlations (modified Wallis correlation, Alipchenkov et al. correlation, Levitan correlation and Stevanovic et al. correlation), the predictions of Stevanovic et al. correlation provide better agreement with Kreydin et al. [16] experimental data.

According to Fig. 2, when the total mass flux (inlet mass flux) is lower than 60 kg/m²s (i.e. the total mass flux is in low mass flux limit), the pressure change is positive, and when the total mass flux increases (such that the mass fluxes do not go beyond the ranges of the low mass flux limit), this positive pressure change increases. When the total mass flux (inlet mass flux) is higher than 100 kg/m²s (i.e. the total mass flux is in high mass flux limit), the pressure change is negative, and also when the total mass flux increases, this negative pressure change increases (the positive pressure drop increases).

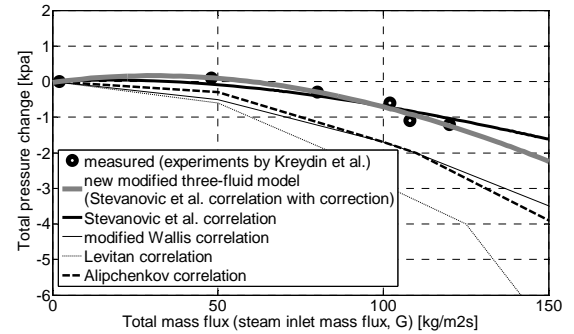


Fig. 2 The modified three-fluid model predictions (Stevanovic et al. correlation with correction) compared with measured data (by Kreydin et al. [16])

If three momentum conservation equations are written and summed up for the three fluids, we have [2]

$$\frac{dp}{dx} = -a_{2W}\tau_{2W} - \rho g \sin \theta - \frac{d}{dx} \left(\sum_{k=1}^3 \alpha_k \rho_k u_k^2 \right) \quad (36)$$

where the two-phase flow density is

$$\rho = \alpha_1 \rho_1 + \alpha_2 \rho_2 + \alpha_3 \rho_3 = \sum_{k=1}^3 \alpha_k \rho_k \quad (37)$$

It means that the total pressure gradient is composed of three terms, namely, frictional, gravitational and acceleration pressure gradients. The first term on the right-hand side of Eq. (36) represents the frictional pressure drop (i.e. the liquid film friction on the wall), the second term represents the gravitational pressure change (for the downward condensing flow in vertical tube the inclination angle is $\theta = -\pi/2$), and the third term represents the acceleration pressure change (the pressure change due to the acceleration or deceleration of the flow in the tube).

The calculated total pressure change and its three terms, frictional, gravitational and acceleration pressure changes are also plotted against the total mass flux for steam inlet pressure of 1.08 MPa in Fig. 3. It can be seen that for lower mass fluxes (lower than 60 kg/m²s) the gravitational pressure change is dominant, and as a result

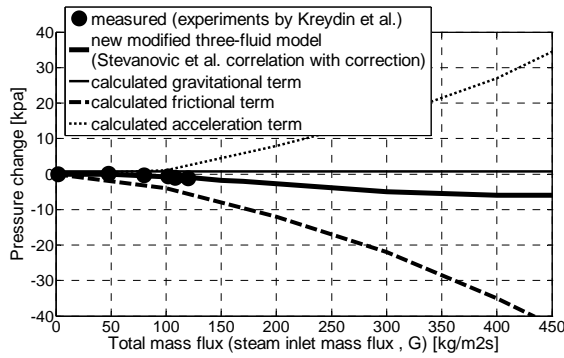


Fig. 3 The modified three-fluid model predictions (Stevanovic et al. correlation with correction) compared with measured data (by Kreydin et al. [16]) along with pressure change terms

of that the pressure increases from the tube inlet to outlet (the gravitational pressure change term, for a downward condensing flow in vertical tube, will be $\Delta p_g = (-\rho g \sin \theta)L = \rho g L$ in the total pressure change and therefore it results in the increase of total pressure change), which gives the reason for the total pressure change being positive in Fig. 2 in the low mass flux limit. For higher mass fluxes (higher than $100 \text{ kg/m}^2\text{s}$) the frictional pressure change is dominant, and consequently the pressure decreases from the tube inlet to outlet (the value of the frictional pressure change term is $\Delta p_f = (-a_{2W} \tau_{2W})L \leq 0$ in the total pressure change, and therefore it results in the decrease of total pressure change), which gives the reason for total pressure change being negative in Fig. 2 in the high mass flux limit.

In condensing vertical tubes, there should be enough pressure drops in order to remove the condensate from the tube outlet. Therefore, the aim is to have a negative pressure change (or a positive pressure drop). With the help of Figs. 2 and 3, we can figure out the range of the total mass flux for which the pressure change is negative (or the pressure drop is positive), and therefore choose a value of the mass flux for the vertical condensing tube for which there is a negative pressure change. In fact, in the industrial applications of the vertical condensing tubes, which are the various heat exchangers in power and chemical industry such as air heaters in steam boilers, air-cooled condensers, and steam condensers within the passive systems of nuclear power plants, we need an inlet mass flux for a specified value of the total pressure drop. Figs. 2 and 3 can help to obtain the values of inlet mass fluxes with the modified three-fluid model giving the best results.

4. Conclusions

The pressure changes of condensing annular flow in vertical tube have been predicted using three-fluid model. Use of the previous correlations for the steam-liquid film interfacial friction shows discrepancies between calculated and measured pressure changes. Although the correlation of Stevanovic et al. [2] provides good agreement, it has some deficiencies. One of these deficiencies corrected in this paper is the introduction of the friction stress between entrained droplets and liquid film. In this study, the calculated pressure changes provide even much

better agreement by taking the above correction into account such that the agreement of the predictions of the modified three-fluid model with measured data is 30% better than the agreement of the predictions of Stevanovic et al. correlation with measured data.

The conservation equations are written for each fluid and then steady one-dimensional conditions are considered. Apart from nine conservation equations (mass, momentum and energy equations for $k = 1, 2, 3$), another equation (volume fraction equation) is also obtained. These ten equations are used to obtain ten state variables. In the conservation equations, the interfacial transfer phenomena are calculated by suitable closure relations.

The conservation equations along with volume fraction equation are changed by some arithmetic operations to ten first-order ODEs which give the derivatives of ten state variables. These ten ODEs comprise a system of stiff ODEs which should be solved together as they are coupled. Here for the solution of the system of stiff ODEs MATLAB stiff ODE solvers, namely ode23s and ode15s, are used. The results obtained are as follows.

1. The modified three-fluid model (Stevanovic et al. correlation with correction - introduction of friction stress of droplets with liquid film) provides much better agreement with measured data compared with other correlations. The main difference between the modified three-fluid model and Stevanovic et al. correlation is in the region with total mass fluxes higher than $120 \text{ kg/m}^2\text{s}$, where the modified three-fluid model predicts higher total pressure changes than Stevanovic et al. correlation.

2. When the total mass flux is in low mass flux limit, the pressure change is positive, and when the mass flux increases, this positive pressure change increases. When the total mass flux is in high mass flux limit, the pressure change is negative, and when the total mass flux increases, this negative pressure change increases.

3. For lower mass fluxes (lower than $60 \text{ kg/m}^2\text{s}$) the gravitational pressure change is dominant, and as a result of that the pressure increases from the tube inlet to outlet. For higher mass fluxes (higher than $100 \text{ kg/m}^2\text{s}$) the frictional pressure change is dominant, and consequently the pressure decreases from the tube inlet to outlet.

4. For the applications of the vertical condensing tubes in industry, the inlet mass flux is needed for a specified value of the total pressure change, for which the modified three-fluid model can be used giving the best results.

References

1. **Ghiaasiaan, S.M.** 2008. Two-Phase Flow, Boiling and Condensation in Conventional and Miniature Systems, 1st Edition. Cambridge University Press. 613p.
2. **Stevanovic, V.D.; Stanojevic, M.; Radic, D.; Jovanovic, M.** 2008. Three-fluid model predictions of pressure changes in condensing vertical tubes, Int. J. of Heat and Mass Transfer 51: 3736-3744.
3. **Sugawara, S. and Miyamoto, Y.** 1990. FIDAS: Detailed sub-channel analysis code on the three-fluid and three-field model, Nuclear Engineering and Design 120: 147-161.
4. **White, F.M.** 1991. Viscous Fluid Flow. New York: McGraw-Hill. 422p.
5. **Sinkunas, S.; Kiela, A.** 2010. Effect of liquid physical properties variability on film thickness, Mechanika

- 1(81): 25-29.
6. **Wallis, G.B.** 1969. One-Dimensional Two-Phase Flow. New York: McGraw-Hill. 322p.
 7. **Alipchenkov, V.M.; Nigmatulin, R.I.; Soloviev, S.L.; Stonik, O.G.; Zaichik, L.I.; and Zeigarnik, Y.A.** 2004. A three-fluid model of two-phase dispersed-annular flow, *Int. J. of Heat and Mass Transfer* 47: 5323-5338.
 8. **Levitan, L.L.** 1987. Dry-out in annular-dispersed flow, *Advances in thermal-hydraulics of two-phase flows in energy plants*. Moscow: Nauka. 146p. (in Russian).
 9. **Clift, R.; Grace, J.R.; Weber, M.E.** 1978. Bubbles, Drops and Particles. New York: Academic Press. 111p.
 10. **Sugawara, S.** 1990. Droplet deposition and entrainment modeling based on the three-fluid model, *Nuclear Engineering and Design* 122: 67-84.
 11. **Downar-Zapolski, Z.; Bilicki, Z.; Bolle, L. and Franco, J.** 1996. The non-equilibrium relaxation model for one-dimensional flashing liquid flow, *Int. J. of Multiphase Flow* 22: 473-483.
 12. **Sinkunas, S.; Kiela, A.** 2009. Effect of temperature gradient on heat transfer and friction in laminar liquid film, *Mechanika* 1(75): 31-35.
 13. **Hazuku, T.; Takamasa, T.; Hibiki, T.; Ishii, M.** 2007. Interfacial area concentration in annular two-phase flow, *Int. J. of Heat and Mass Transfer* 50: 2986-2995.
 14. **Hinze, J.O.** 1975. Turbulence. New York: McGraw-Hill. 453p.
 15. **Zaichik, L.I. and Alipchenkov, V.M.** 1999. Interaction time of turbulent eddies and colliding particles, *Thermophys. Aeromech.* 6: 493-501.
 16. **Kreydin, B.L.; Kreydin, I.L.; Lokshin, V.A.** 1985. Experimental research of the total pressure drop in the condensing steam downward flow inside a vertical tube, *Therm. Eng.* 32(7): 42-43 (in Russian).

H. Saffari, N. Dalir

LAŠELIŲ IR PLĖVELĖS TARPUSAVIO TRINTIES ĮTEMPIŲ EFEKTAS PROGNOZUOJANT SLĖGIO POKYČIUS KONDENSACINIULOSE VAMZDŽIUOSE

R e z i ū m ė

Slėgio pokyčiai esant kondensaciniam apskritimui tekėjimui vertikaliuose vamzdžiuose gali būti prognozuojami naudojant Stevanovičiaus ir kitų trijų skysčių modelį. Garo ir skysčio plėvelės paviršių tarpusavio trinties nustatyti naudojant ankstesnes koreliacijas apskaičiuoto ir išmatuoto (eksperimentinio) slėgio pokyčiai nesutapo. Nors Stevanovičiaus ir kitų siūloma koreliacija gerai sutampa, ji turi ir trūkumų. Vienam iš trūkumų pašalinti šiame darbe yra panaudoti trinties įtempiai tarp apkrautų lašelių (dispersijos fazė) ir skysčio plėvelės. Įvertinus šią korekciją apskaičiuoti slėgio pokyčiai geriau sutampa su išmatuotais. Buvo analizuota frikcinė, gravitacinė ir slėgio pokyčių pagreičio įtaka bendram slėgio pokyčiui. Taip pat buvo nustatytas lašelių apkrovimas ir nusėdimas.

H. Saffari, N. Dalir

EFFECT OF FRICTION STRESS OF DROPLETS WITH FILM ON PREDICTION OF PRESSURE CHANGES IN CONDENSING TUBES

S u m m a r y

The pressure changes of condensing annular flow in vertical tubes have been predicted using three-fluid model. Use of the previous correlations for the steam-liquid film interfacial friction shows discrepancies between calculated and measured (experimental) pressure changes. Although the correlation of Stevanovic et al. provides good agreement, it has some deficiencies. One of these deficiencies corrected in this paper is introduction of the friction stress between entrained droplets (dispersed phase) and liquid film. Calculated pressure changes provide even much better agreement with measured data by taking the above correction into account such that the agreement of the predictions of the modified three-fluid model with experimental data is 30% better than the agreement of the predictions of Stevanovic et al. correlation with experimental data. The influence of frictional, gravitational and acceleration pressure changes on total pressure change has been analyzed. The entrainment and deposition of droplets has also been considered.

Х. Саффари, Н. Далир

ЭФФЕКТ НАПРЯЖЕНИЙ ТРЕНИЯ МЕЖДУ КАПЛЯМИ И ПЛЕНКОЙ ПРИ ПРОГНОЗИРОВАНИИ ИЗМЕНЕНИЙ ДАВЛЕНИЯ В КОНДЕНСАЦИОННЫХ ТРУБАХ

Р е з ю м е

Изменения давления при конденсационном круговом течении в вертикальных трубах прогнозировались при помощи модели жидкостей Стевановича и трех других. При использовании прежних корреляций для определения междуповерхностного трения пара и пленки жидкости получено несоответствие между расчетном и измеренном (экспериментальном) изменении давления. Хотя предлагаемая Стевановичем и другими корреляция дает хорошее соответствие, оно имеет и несколько недостатков. Для устранения одного из недостатков в этой работе использованы напряжения трения между нагруженными каплями (фаза дисперсии) и пленкой жидкости. После применения этой коррекции расчетное изменение давления дает значительно лучшее соответствие. Рассмотрено влияние фрикционных, гидравлических изменений и изменения ускорения давления на общее изменение давления. Также было определена нагрузка и осадка капель.

Received August 03, 2010

Accepted January 17, 2011